# Quark mass dependence of masses and decay constants of the pseudo-Goldstone bosons in QCD

The $qq+q$ Collaboration

F. Farchioni[1], I. Montvay[2], E. Scholz[2], L. Scorzato[2]

[1] Westfälische Wilhelms-Universität Münster, Institut für Theoretische Physik, Wilhelm-Klemm-Strasse 9, 48149 Münster, Germany
[2] Deutsches Elektronen-Synchrotron DESY, Notkestr. 85, 22603 Hamburg, Germany

**Abstract.** The dependence of the pseudo-scalar meson masses and decay constants on sea and valence quark masses is compared to next-to-leading order (NLO) chiral perturbation theory (ChPT). The numerical simulations with two light dynamical quark flavors are performed with the Wilson quark lattice action at gauge coupling $\beta = 5.1$ and hopping parameters $\kappa = 0.176, 0.1765, 0.177$ on a $16^4$ lattice. $\mathcal{O}(a)$ lattice artifacts are taken into account by applying chiral perturbation theory for the Wilson lattice action. The values of the relevant combinations of Gasser–Leutwyler constants $L_4$, $L_5$, $L_6$ and $L_8$ are estimated.

## 1 Introduction

The low energy dynamics of strong interactions in the pseudo-Goldstone boson sector of QCD is constrained by the non-linear realization of spontaneously broken chiral symmetry [1]. In an expansion in powers of momenta and light quark masses a few low energy constants – the Gasser–Leutwyler constants – appear which parameterize the strength of interactions in the low energy chiral Lagrangian [2]. The Gasser–Leutwyler constants are free parameters which can be constrained by analyzing experimental data. In the framework of lattice regularization they can be determined from first principles by numerical simulations. In experiments one can investigate processes with different momenta but the quark masses are, of course, fixed by nature. In numerical simulations there is, in principle, much more freedom because, besides the possibility of changing momenta, one can also freely change the masses of the quarks. This allows for a precise determination of the Gasser–Leutwyler constants – once the simulations reach high precision. First steps towards this goal have recently been done by several authors [3–6] including our Collaboration [7–9].

The main difficulty for numerical simulations in lattice QCD is to reach the regime of light quark masses where ChPT is applicable. The reason is the critical slowing down of simulation algorithms for small quark masses and lattice spacings. We apply the two-step multi-boson (TSMB) algorithm [10] which allows one to perform simulations with small quark masses within the range of applicability of next-to-leading order (NLO) ChPT [7,8].

Another important aspect of investigating the quark mass dependence in numerical simulations is the possibility to use ChPT for the extrapolation of the results to the physical values of $u$- and $d$-quark masses which would be very difficult to reach otherwise. In fact, ChPT can be extended by changing the *valence quark masses* in quark propagators independently from the *sea quark masses* in virtual quark loops which are represented in the path integral by the *quark determinant*. In this way one arrives at partially quenched chiral perturbation theory (PQChPT) [11–13]. The freedom of changing valence and sea quark masses substantially contributes to the power of lattice QCD both in performing quark mass extrapolations and in determining the values of the Gasser–Leutwyler constants [14].

For a fast convergence of numerical results to the continuum limit it is important to explicitly deal with the leading $\mathcal{O}(a)$ lattice artifacts. An often used method is the application of the $\mathcal{O}(a)$ improved lattice action [15]. We apply an alternative technique [16] which in the pseudo-Goldstone boson sector is equivalent to the $\mathcal{O}(a)$ improvement of the lattice action. In this method the (unimproved) Wilson action is used in the Monte Carlo generation of gauge configurations and the $\mathcal{O}(a)$ effects are compensated in PQChPT itself. This means that we apply *chiral perturbation theory for the Wilson lattice action*. Our calculations showed that in practice this method gives results with good precision [9].

The plan of this paper is as follows: in the next two sections we collect the NLO (PQ)ChPT formulas for ratios of pseudo-scalar meson masses and decay constants. In Sect. 2 a discussion of the general form of the NNLO tree-

graph corrections is also included. In Sect. 4 the results of numerical simulations is presented. The last section is devoted to a summary and discussion.

## 2 Valence quark mass dependence

In this paper we use the notation introduced in [9] which slightly differ from those of [14,16]. The dimensionless variables for quark masses and $\mathcal{O}(a)$ lattice artifacts are denoted, respectively, by

$$\chi_A \equiv \frac{2B_0 m_q}{f_0^2} , \qquad \rho_A \equiv \frac{2W_0 a c_{\mathrm{SW}}}{f_0^2} . \qquad (1)$$

Here $m_q$ is the quark mass, $a$ the lattice spacing, $B_0$ and $W_0$ are parameters of dimension mass and (mass)$^3$, respectively, which appear in the leading order (LO) chiral effective Lagrangian, $c_{\mathrm{SW}}$ is the coefficient of the $\mathcal{O}(a)$ chiral symmetry breaking term and $f_0$ is the value of the pion decay constant at zero quark mass. (Its normalization is such that the physical value is $f_0 \simeq 93\,\mathrm{MeV}$.) For fixed sea quark mass $\chi_{\mathrm{S}}$ the dependence of the pseudo-scalar meson mass and decay constant on the valence quark mass $\chi_{\mathrm{SV}}$ can be described by the variables

$$\xi \equiv \frac{\chi_{\mathrm{SV}}}{\chi_{\mathrm{S}}} , \qquad \eta_{\mathrm{S}} \equiv \frac{\rho_{\mathrm{S}}}{\chi_{\mathrm{S}}} . \qquad (2)$$

For instance, in case of a number of $N_{\mathrm{s}}$ equal mass sea quarks the ratios of decay constants are given by

$$\begin{aligned}
Rf_{\mathrm{VV}} \equiv \frac{f_{\mathrm{VV}}}{f_{\mathrm{SS}}} &= 1 + 4(\xi - 1)\chi_{\mathrm{S}} L_{\mathrm{S}5} \\
&- \frac{N_{\mathrm{s}}\chi_{\mathrm{S}}}{64\pi^2}(1 + \xi + 2\eta_{\mathrm{S}}) \log \frac{1 + \xi + 2\eta_{\mathrm{S}}}{2} \\
&+ \frac{N_{\mathrm{s}}\chi_{\mathrm{S}}}{32\pi^2}(1 + \eta_{\mathrm{S}}) \log(1 + \eta_{\mathrm{S}}) ,
\end{aligned} \qquad (3)$$

and similarly

$$\begin{aligned}
Rf_{\mathrm{VS}} \equiv \frac{f_{\mathrm{VS}}}{f_{\mathrm{SS}}} &= 1 + 2(\xi - 1)\chi_{\mathrm{S}} L_{\mathrm{S}5} \\
&+ \frac{\chi_{\mathrm{S}}}{64N_{\mathrm{s}}\pi^2}(\xi - 1) - \frac{\chi_{\mathrm{S}}}{64N_{\mathrm{s}}\pi^2}(1 + \eta_{\mathrm{S}}) \log \frac{\xi + \eta_{\mathrm{S}}}{1 + \eta_{\mathrm{S}}} \\
&- \frac{N_{\mathrm{s}}\chi_{\mathrm{S}}}{128\pi^2}(1 + \xi + 2\eta_{\mathrm{S}}) \log \frac{1 + \xi + 2\eta_{\mathrm{S}}}{2} \\
&+ \frac{N_{\mathrm{s}}\chi_{\mathrm{S}}}{64\pi^2}(1 + \eta_{\mathrm{S}}) \log(1 + \eta_{\mathrm{S}}) .
\end{aligned} \qquad (4)$$

$L_{\mathrm{S}k}$ $(k = 5)$ denotes the relevant Gasser–Leutwyler coefficient at the scale $f_0\sqrt{\chi_{\mathrm{S}}}$. This is related to $\bar{L}_k$ defined at the scale $f_0$ and $L'_k$ defined at the generic scale $\mu$ according to

$$L_{\mathrm{S}k} = \bar{L}_k - c_k \log(\chi_{\mathrm{S}}) = L'_k - c_k \log \left( \frac{f_0^2}{\mu^2} \chi_{\mathrm{S}} \right) . \qquad (5)$$

with the constants $c_k$ $(k = 4, 5, 6, 8)$ given below. Similarly, the corresponding relations for the coefficients $W_{\mathrm{S}k}$ introduced in [16] are

$$W_{\mathrm{S}k} = \bar{W}_k - d_k \log(\chi_{\mathrm{S}}) = W'_k - d_k \log \left( \frac{f_0^2}{\mu^2} \chi_{\mathrm{S}} \right) . \qquad (6)$$

The constants in (5) and (6) are given by

$$c_4 = \frac{1}{256\pi^2} , \qquad c_5 = \frac{N_{\mathrm{s}}}{256\pi^2} ,$$

$$c_6 = \frac{(N_{\mathrm{s}}^2 + 2)}{512N_{\mathrm{s}}^2\pi^2} , \qquad c_8 = \frac{(N_{\mathrm{s}}^2 - 4)}{512N_{\mathrm{s}}\pi^2} , \qquad (7)$$

respectively,

$$d_4 = \frac{1}{256\pi^2} , \qquad d_5 = \frac{N_{\mathrm{s}}}{256\pi^2} ,$$

$$d_6 = \frac{(N_{\mathrm{s}}^2 + 2)}{256N_{\mathrm{s}}^2\pi^2} , \qquad d_8 = \frac{(N_{\mathrm{s}}^2 - 4)}{256N_{\mathrm{s}}\pi^2} . \qquad (8)$$

For the valence quark mass dependence of the (squared) pseudo-scalar meson masses one can consider, similarly to (3) and (4), the ratios

$$Rm_{\mathrm{VV}} \equiv \frac{m_{\mathrm{VV}}^2}{m_{\mathrm{SS}}^2} , \qquad Rm_{\mathrm{VS}} \equiv \frac{m_{\mathrm{VS}}^2}{m_{\mathrm{SS}}^2} . \qquad (9)$$

In the present paper we prefer to divide these ratios by the tree level dependences and consider

$$\begin{aligned}
Rn_{\mathrm{VV}} \equiv \frac{m_{\mathrm{VV}}^2}{\xi m_{\mathrm{SS}}^2} &= 1 - \eta_{\mathrm{S}} \frac{(\xi - 1)}{\xi} \\
&+ 8(\xi - 1)\chi_{\mathrm{S}}(2L_{\mathrm{S}8} - L_{\mathrm{S}5}) \\
&+ 8N_{\mathrm{s}} \frac{(\xi - 1)}{\xi} \eta_{\mathrm{S}}\chi_{\mathrm{S}}(L_{\mathrm{S}4} - W_{\mathrm{S}6}) \\
&+ \frac{\chi_{\mathrm{S}}}{16N_{\mathrm{s}}\pi^2} \frac{(\xi - 1)}{\xi}(\xi + \eta_{\mathrm{S}}) \\
&- \frac{\chi_{\mathrm{S}}}{16N_{\mathrm{s}}\pi^2}(1 + 2\eta_{\mathrm{S}}) \log(1 + \eta_{\mathrm{S}}) \\
&+ \frac{\chi_{\mathrm{S}}}{16N_{\mathrm{s}}\pi^2} \frac{(2\xi^2 - \xi - \eta_{\mathrm{S}} + 3\eta_{\mathrm{S}}\xi)}{\xi} \log(\xi + \eta_{\mathrm{S}}) ,
\end{aligned} \qquad (10)$$

and

$$\begin{aligned}
Rn_{\mathrm{VS}} \equiv \frac{2m_{\mathrm{VS}}^2}{(\xi + 1)m_{\mathrm{SS}}^2} &= 1 - \eta_{\mathrm{S}} \frac{(\xi - 1)}{(\xi + 1)} \\
&+ 4(\xi - 1)\chi_{\mathrm{S}}(2L_{\mathrm{S}8} - L_{\mathrm{S}5}) \\
&+ 8N_{\mathrm{s}} \frac{(\xi - 1)}{(\xi + 1)} \eta_{\mathrm{S}}\chi_{\mathrm{S}}(L_{\mathrm{S}4} - W_{\mathrm{S}6}) \\
&- \frac{\chi_{\mathrm{S}}}{16N_{\mathrm{s}}\pi^2}(1 + 2\eta_{\mathrm{S}}) \log(1 + \eta_{\mathrm{S}}) \\
&+ \frac{\chi_{\mathrm{S}}}{16N_{\mathrm{s}}\pi^2} \frac{(\xi^2 + \xi + \eta_{\mathrm{S}} + 3\eta_{\mathrm{S}}\xi)}{(\xi + 1)} \log(\xi + \eta_{\mathrm{S}}) .
\end{aligned} \qquad (11)$$

A useful quantity is the double ratio of decay constants [17] which does not depend on any of the NLO coefficients. In other words there one can see the chiral logarithms alone. The NLO expansion for this quantity is

$$RRf \equiv \frac{f_{VS}^2}{f_{VV}f_{SS}} = 1 + \frac{\chi_S}{32N_s\pi^2}(\xi-1)$$

$$-\frac{\chi_S}{32N_s\pi^2}(1+\eta_S)\log\frac{\xi+\eta_S}{1+\eta_S} . \tag{12}$$

The double ratio of the pion mass squares [18] corresponding to (10) and (11) has the NLO expansion

$$RRn \equiv \frac{4\xi m_{VS}^4}{(\xi+1)^2 m_{VV}^2 m_{SS}^2} = 1 - \frac{\eta_S(\xi-1)^2}{\xi(\xi+1)}$$

$$+\frac{\chi_S(\xi^2+\xi+\eta_S+3\eta_S\xi^2)\log(\xi+\eta_S)}{16N_s\pi^2\xi(\xi+1)}$$

$$-\frac{\chi_S(2\eta_S+1)\log(1+\eta_S)}{16N_s\pi^2}$$

$$-\frac{\chi_S(\xi-1)(\xi+\eta_S)}{16N_s\pi^2\xi}$$

$$+\frac{8N_s\chi_S\eta_S(\xi-1)^2}{\xi(\xi+1)}(L_{S4}-W_{S6}) . \tag{13}$$

## 2.1 Quadratic corrections

A complete NNLO (i. e. two-loop) calculation in PQChPT for our physical quantities is not yet available. Nevertheless, the general form of NNLO tree-graph ("counterterm insertion") contributions can be given [19][1]. For instance, one has for the pion mass square:

$$\frac{\delta m_{AB}^2}{m_{AB}^2} = \alpha_1\chi_S^2 + \alpha_2\chi_S(\chi_A+\chi_B)$$

$$+\alpha_3(\chi_A+\chi_B)^2 + \alpha_4(\chi_A^2+\chi_B^2) . \tag{14}$$

(Here $A$ and $B$ denote generic quark indices: S is the label for the sea quarks, V for valence quarks.) For the pion decay constant there is a similar expression. This information is very useful in order to estimate the importance of the NNLO terms in our present range of quark masses.

The general characteristic of the NNLO terms is that they are proportional to the quark mass square: $\chi_S^2$. (Here we only consider terms in the continuum limit and hence neglect lattice artifacts. This will be to some extent justified a posteriori by the observed smallness of the $\mathcal{O}(a)$ terms.) Neglecting loop contributions, which are at the NLO order relatively small, the dependence on the quark mass ratio $\xi$ is at most quadratic and can, therefore, be represented by terms proportional to $(\xi-1)$ and $(\xi-1)^2$. Therefore, these contributions have the generic form

$$D_X\chi_S^2(\xi-1) + Q_X\chi_S^2(\xi-1)^2 . \tag{15}$$

[1] We thank the authors for communicating us the content of this paper prior to publication

Here $X$ denotes an index specifying the considered ratio as, for instance, $X = fVV$, $nVS$ etc. for the single ratios and $X = fd$ and $X = nd$ for the double ratios $RRf$ and $RRn$, respectively. The NLO tree-graph contributions for the single ratios $Rf$ and $Rn$ are also proportional to $(\xi-1)$. These can be parametrized as $L_X\chi_S(\xi-1)$ (for instance, we have $L_{fVV} \equiv 4L_5$ and $L_{nVV} \equiv 8(2L_8-L_5)$). The inclusion of $D_X$-type terms is equivalent to a linear dependence of the effective $L_X$ for fixed $\chi_S$:

$$L_X^{\text{eff}} = L_X + D_X\chi_S . \tag{16}$$

At this point one has to remember that mathematically speaking – in order to completely remove the effect of higher order terms – $L_X$ is defined in the limit $\chi_S \to 0$.

The NNLO coefficients are not all independent but satisfy the relations

$$D_{fVS} = \frac{1}{2}D_{fVV} , \qquad D_{nVS} = \frac{1}{2}D_{nVV} ,$$

$$D_{fd} = 0 , \qquad D_{nd} = 0 ,$$

$$Q_{fd} = 2Q_{fVS} - Q_{fVV} + \frac{1}{4}L_{fVV}^2 ,$$

$$Q_{nd} = 2Q_{nVS} - Q_{nVV} + \frac{1}{4}L_{nVV}^2 . \tag{17}$$

The first line is a consequence of the general structure of the NNLO tree-graph contributions. The last two lines follow from the definition of $RRf$ and $RRn$ if one only considers NLO and NNLO tree-graph contributions.

We shall see in Sect. 4 that in our range of quark masses the NNLO tree-graph contributions of the form (15) are important but can be approximately determined by global fits. In this way the NLO constants $L_k$ are better determined. Observe that a determination of the $D_X$ is only possible in our analysis if different sea quark masses are included (see below).

## 2.2 $\mathcal{O}(a^2)$ corrections

The idea of including leading lattice artifacts in the low energy effective Lagrangian for the Wilson lattice action can be extended to higher orders in lattice spacing. Indeed, in writing this paper we have seen two recent publications about the inclusion of $\mathcal{O}(a^2)$ corrections [20, 21]. The general formulas derived in these papers for the $\mathcal{O}(a^2)$ terms imply that in the formulas for the pion mass-squared ratios (10), (11) and (13) there are only very little changes. In fact, the changes can be summarized by the replacement

$$\eta_S(L_{S4}-W_{S6}) \longrightarrow \eta_S(L_{S4}-W_{S6})$$

$$+ \frac{\eta_S^2}{N_s}(N_sW_{S4}+W_{S5}-2N_sW_{S6}'-2W_{S8}') . \tag{18}$$

Here $W_{S6}'$ and $W_{S8}'$ denote some new low energy constants appearing in the $\mathcal{O}(a^2)$ part of the effective Lagrangian. This means that fitting the valence quark mass

dependence with our formulas (10), (11) and (13) effectively takes into account also $\mathcal{O}(a^2)$ corrections.

Concerning the ratios of the pion decay constants in (3), (4) and (12) the situation is expected to be similar but there, in addition to the $\mathcal{O}(a^2)$ terms, also new types of $\mathcal{O}(am_q)$ terms may appear.

## 3 Sea quark mass dependence

The dependence on the sea quark mass can be treated similarly to the valence quark mass dependence considered in Sect. 2. Here one chooses a "reference value" of the sea quark mass $\chi_R$ and determines the ratios of the coupling and decay constant as a function of

$$\sigma \equiv \frac{\chi_S}{\chi_R} , \qquad \tau \equiv \frac{\rho_S}{\rho_R} . \qquad (19)$$

Instead of $\tau$ one can also use

$$\eta_S \equiv \frac{\rho_S}{\chi_S} , \qquad \eta_R \equiv \frac{\rho_R}{\chi_R}, \qquad (20)$$

which satisfy

$$\frac{\tau}{\sigma} = \frac{\eta_S}{\eta_R} . \qquad (21)$$

With this we have for the decay constants

$$\begin{aligned} Rf_{SS} \equiv \frac{f_{SS}}{f_{RR}} &= 1 + 4(\sigma - 1)\chi_R(N_s L_{R4} + L_{R5}) \\ &+ 4(\eta_S\sigma - \eta_R)\chi_R(N_s W_{R4} + W_{R5}) \\ &- \frac{N_s\chi_R}{32\pi^2}\sigma(1 + \eta_S)\log[\sigma(1 + \eta_S)] \\ &+ \frac{N_s\chi_R}{32\pi^2}(1 + \eta_R)\log(1 + \eta_R) \end{aligned} \qquad (22)$$

and for the mass squares

$$\begin{aligned} Rn_{SS} \equiv \frac{m_{SS}^2}{\sigma m_{RR}^2} &= 1 + \eta_S - \eta_R \\ &+ 8(\sigma - 1)\chi_R(2N_s L_{R6} + 2L_{R8} - N_s L_{R4} - L_{R5}) \\ &+ 8(\eta_S\sigma - \eta_R)\chi_R(2N_s W_{R6} + 2W_{R8} \\ &\quad - N_s W_{R4} - W_{R5} - N_s L_{R4} - L_{R5}) \\ &+ \frac{\chi_R}{16\pi^2 N_s}\sigma(1 + 2\eta_S)\log[\sigma(1 + \eta_S)] \\ &- \frac{\chi_R}{16\pi^2 N_s}(1 + 2\eta_R)\log(1 + \eta_R) . \end{aligned} \qquad (23)$$

Of course, the coefficients $L_{Rk}$ and $W_{Rk}$ ($k = 4, 5, 6, 8$) are now defined at the scale $f_0\sqrt{\chi_R}$ therefore in the relations (5) and (6) $\chi_S$ is replaced by $\chi_R$.

The logarithmic dependence of the $L_{Sk}$ and $W_{Sk}$ have to be taken into account also in simultaneous fits of the valence quark mass dependence at several sea quark mass values. Choosing a fixed *reference sea quark mass* $\chi_R$ we have from (5) and (6) with $\mu = f_0\sqrt{\chi_R}$

$$L_{Sk} = L_{Rk} - c_k \log\sigma , \qquad W_{Sk} = W_{Rk} - d_k \log\sigma . \qquad (24)$$

The NLO PQChPT formulas for the valence quark mass dependence in terms of the reference sea quark mass are obtained by the following substitutions in (3), (4), (10)–(13):

$$\begin{aligned} \chi_S \to \sigma\chi_R , \quad L_{Sk} &\to L_{Rk} , \quad W_{Sk} \to W_{Rk} , \\ \log(1 + \eta_S) &\to \log[\sigma(1 + \eta_S)] , \\ \log(\xi + \eta_S) &\to \log[\sigma(\xi + \eta_S)] , \\ \log(1 + \xi + 2\eta_S) &\to \log[\sigma(1 + \xi + 2\eta_S)] . \end{aligned} \qquad (25)$$

An important feature of both the valence and sea quark mass dependences considered in the present work is that they are ratios taken at a fixed value of the gauge coupling ($\beta$). These are renormalization group invariants independent from the $Z$-factors of multiplicative renormalization since the $Z$-factors only depend on the gauge coupling and not on the quark mass. Taking ratios of pion mass squares and pion decay constants at varying quark masses has, in general, the advantage that quark mass independent corrections – for instance of $\mathcal{O}(a)$ and/or $\mathcal{O}(a^2)$ – cancel.

## 4 Numerical simulations

We performed Monte Carlo simulations with $N_s = 2$ degenerate sea quarks on a $16^4$ lattice at $\beta = 5.1$ and three values of $\kappa$: $\kappa_0 = 0.176$, $\kappa_1 = 0.1765$ and $\kappa_2 = 0.177$. For the *reference sea quark mass* we choose $\kappa_R \equiv \kappa_0 = 0.176$. A summary of the simulation points is reported in Table 1, where also the set-up of the TSMB algorithm for the different simulation points can be found. The gauge field configurations collected for the evaluation of the physical quantities are separated by 10 TSMB update cycles consisting out of boson field and gauge field updates and noisy correction steps. It turned out that these configurations were statistically independent from the point of view of almost all secondary quantities considered. Exceptions are $r_0/a$ and $M_r$ (see below) where autocorrelation lengths of 2–5 units in the configuration sequences appear.

We investigated for each simulation point the valence quark mass dependence of the pseudo-Goldstone boson spectrum and decay constants; the values of the valence $\kappa$ considered for each simulation point are reported in Table 2. In these intervals the valence quark masses are approximately changing in the range $\frac{1}{2}m_{sea} \leq m_{valence} \leq 2m_{sea}$.

A rough estimate of the sea quark mass range can be obtained by considering the quantity $M_r \equiv (r_0 m_\pi)^2$, which for the strange quark gives $M_r \approx 3.1$. (Here $r_0 \approx 0.5\,\text{fm}$ is the Sommer scale parameter which characterizes the distance scale intrinsic to the gauge field.) In our simulation points the value of $M_r$ ranges between $M_r \approx 2.10$ and $M_r \approx 1.09$, corresponding to about $\frac{2}{3}$ and $\frac{1}{3}$ of the

**Table 1.** Parameters of the simulations: all simulations were done at $\beta = 5.10$ with determinant breakup $N_f = 1 + 1$. The other TSMB-parameters are the interval of polynomial approximasions $[\epsilon, \lambda]$ and the polynomial orders $n_{1,2,3}$ [10]

| Run | $\kappa$ | Configurations | $\epsilon$ | $\lambda$ | $n_1$ | $n_2$ | $n_3$ |
|-----|----------|----------------|------------|-----------|-------|-------|-------|
| 0 | 0.1760 | 1811 | $4.50 \cdot 10^{-4}$ | 3.0 | 40 | 210 | 220 |
| 1 | 0.1765 | 746 | $2.50 \cdot 10^{-4}$ | 3.0 | 40–44 | 280 | 260–340 |
| 2 | 0.1770 | 1031 | $3.75 \cdot 10^{-5}$ | 3.0 | 54 | 690 | 840 |

**Table 2.** Values of the valence quark hopping parameter

| Run | 0 | 1 | 2 |
|-----|--------|--------|--------|
| $\kappa_{\text{sea}}$ | 0.1760 | 0.1765 | 0.1770 |
| $\kappa_{\text{valence}}$ | 0.1685 | 0.1710 | 0.1743 |
| | 0.1705 | 0.1718 | 0.1747 |
| | 0.1720 | 0.1726 | 0.1751 |
| | 0.1730 | 0.1734 | 0.1754 |
| | 0.1735 | 0.1742 | 0.1759 |
| | 0.1745 | 0.1750 | 0.1763 |
| | 0.1750 | 0.1758 | 0.1767 |
| | 0.1770 | 0.1772 | 0.1775 |
| | 0.1775 | 0.1778 | 0.1779 |
| | 0.1785 | 0.1785 | 0.1783 |
| | 0.1790 | 0.1791 | 0.1787 |
| | 0.1800 | 0.1797 | 0.1791 |

**Table 3.** The values of some basic quantities in our simulation points. Statistical errors in last digits are given in parentheses. We define $M_r = (r_0 m_\pi)^2$ and $\sigma_i = m_{qi}/m_{q0}$

| $\kappa$ | $\kappa_0$ | $\kappa_1$ | $\kappa_2$ |
|----------|------------|------------|------------|
| $r_0/a$ | 2.149(15) | 2.171(88) | 2.395(52) |
| $am_\pi$ | 0.6747(14) | 0.6211(22) | 0.4354(68) |
| $M_r$ | 2.103(26) | 1.824(41) | 1.088(47) |
| $Z_q am_q$ | 0.07472(32) | 0.06247(51) | 0.03087(36) |
| $\sigma_i$ | 1.0 | 0.8361(52) | 0.4132(34) |

value for the strange quark mass. Since the valence quark masses roughly go down to $m_{\text{valence}} \simeq \frac{1}{2} m_{\text{sea}}$, they reach $m_{\text{valence}} \simeq \frac{1}{6} m_s$. In our configuration samples we did not encounter problems with "exceptional gauge configurations" – in spite of the smallness of the valence quark mass. This means that the quark determinant effectively suppresses such configurations.

Standard methods for the extraction of the relevant physical quantities have been applied (a more detailed description is given in our previous paper [7] and in [22]). Statistical errors have been obtained by the *linearization method* [23, 24] which we found more reliable than jackknifing on bin averages.

Within a mass independent scheme of renormalization – defined at zero quark mass – the $Z$-factors of multiplicative renormalization depend only on the gauge coupling ($\beta$) and not on the quark mass ($\kappa$). Similarly, the lattice spacing $a$ is also a function of the gauge coupling alone [25]. Therefore, since our simulation points are at fixed gauge coupling $\beta = 5.1$, the ratios of the sea quark masses can be obtained by taking ratios of the measured bare quark masses in lattice units $Z_q am_q$. Here $Z_q$ is the multiplicative renormalization factor for the quark mass which is the ratio of the $Z$-factors of the pseudo-scalar density and axial-vector current ($Z_q = Z_P/Z_A$) because we determine the quark mass by the PCAC-relation: $m_q \equiv m_q^{\text{PCAC}}$ [7]. (Of course, in the valence quark ratios the factor $Z_q a$ also cancels trivially.) The obtained values of the sea quark mass ratios $\sigma_i \equiv m_{qi}/m_{q0}$ ($i = 1, 2$) are given in Table 3 together with some other basic quantities.

Note that by identifying the quark mass ratios in the ChPT formulas with the ratios of the PCAC quark masses ("axial-vector Ward identity quark masses") one assumes that these two kinds of renormalized quark masses are proportional to each other. As it is shown, for instance, by (48) in [21] this is indeed the case – apart from lattice artifacts of $\mathcal{O}(am_q)$ and $\mathcal{O}(a^2)$. The quark mass independent part of the $\mathcal{O}(a^2)$ terms are cancelled by taking ratios. The remaining quark mass dependent lattice artifacts are neglected in the present paper.

The critical value of the hopping parameter where the quark mass vanishes can be estimated by a quadratic extrapolation using the values of $\sigma_{1,2}$:

$$\sigma_i \equiv \frac{m_{qi}}{m_{q0}} = \frac{(\kappa_i^{-1} - \kappa_{\text{cr}}^{-1}) + d_\sigma(\kappa_i^{-1} - \kappa_{\text{cr}}^{-1})^2}{(\kappa_0^{-1} - \kappa_{\text{cr}}^{-1}) + d_\sigma(\kappa_0^{-1} - \kappa_{\text{cr}}^{-1})^2} \ . \quad (26)$$

The values of $\sigma_{1,2}$ in Table 3 give the solution $\kappa_{\text{cr}} = 0.1773(1)$ and $d_\sigma = -11.2(8)$. (The relatively large absolute value of $d_\sigma$ shows that the quadratic term in the extrapolation is important.)

The value of the lattice spacing $a$ can be inferred from the value of $r_0/a$ at $\kappa = \kappa_{\text{cr}}$. This can also be determined by a quadratic extrapolation of the values of $r_0/a$ given in Table 3 with the result: $r_0(\kappa_{\text{cr}})/a = 2.65(7)$. Taking, by definition, $r_0(\kappa_{\text{cr}}) = 0.5$ fm this gives for the lattice spacing: $a = 0.189(5)$ fm.

The physical volume following from the lattice spacing is comfortably large: $L \simeq 3.0$ fm. Since the minimal value of the pion mass in lattice units in our points is $am_\pi^{\text{min}} \simeq 0.43$ for sea quarks and $am_\pi^{\text{min}} \simeq 0.30$ for the lightest valence quark, we have $Lm_\pi \geq 4.8$.

Another piece of information given by the values of $M_r$ is an estimate of the quark mass parameter $\chi_S$ in the ChPT formulas. For instance, in the reference point we have from $r_0 f_0 \simeq 0.23$ [26]: $\chi_R^{\text{estimate}} \approx M_r/(r_0 f_0)^2 \simeq 39.8$.

## 4.1 Valence quark mass dependence

For a fixed value of the sea quark mass $\chi_S$ the valence quark mass dependence of the ratios $Rf_{VV,VS}$, $Rn_{VV,VS}$, $RRf$ and $RRn$ is determined by five parameters:

$$\chi_S, \quad \eta_S, \quad \chi_S L_{S5},$$

$$\chi_S L_{S4W6} \equiv \chi_S(L_{S4} - W_{S6}),$$

$$\chi_S L_{S85} \equiv \chi_S(2L_{S8} - L_{S5}). \tag{27}$$

The dependence is non-linear in $\eta_S$ and linear in the rest.

After performing such fits of the data we realized that the sea quark mass dependence is not consistent with the NLO PQChPT formulas. In particular, the best fit values of the $\chi_S$ have ratios considerably closer to 1 than $\sigma_{1,2}$ in Table 3 and the change of the $L_k$ with $\chi_S$ is also not consistent with (24). This shows that NNLO effects are important and, therefore, we tried fits including NNLO tree-graph terms of the form given in (15). The list of the relevant NNLO-parameters is

$$\chi_R^2 D_{fVV,nVV}, \quad \chi_R^2 Q_{fVV,fVS,fd,nVV,nVS,nd}. \tag{28}$$

$Q_{fd}$ and $Q_{nd}$ have to satisfy the quadratic relations given in the last line of (17) but in order to keep linearity we did not impose these relations and fitted the eight parameters in (28) independently. After performing the fits one can check how well the relations for $Q_{fd}$ and $Q_{nd}$ are fulfilled.

The global fit of the valence quark mass dependence for several values of the sea quark mass has twelve linear parameters: the linear parameters in (27) with $\chi_S$ replaced by $\chi_R$

$$\chi_R, \quad \chi_R L_{R5},$$

$$\chi_R L_{R85} \equiv \chi_R(2L_{R8} - L_{R5}),$$

$$\chi_R L_{R4W6} \equiv \chi_R(L_{R4} - W_{R6}) \tag{29}$$

and the eight in (28). In addition there are the non-linear parameters, in our case three of them: $\eta_S = \eta_{0,1,2}$.

Multi-parameter linear fits are easy and, except for degenerate situations, the chi-square always has a unique well-defined minimum. Non-linear fits involving the $\eta$ are more problematic; therefore, we adopted the following procedure: performing non-linear fits at individual sea quark mass values we obtained the starting values of $\eta_{0,1,2}$. Then for fixed values of $\eta_{0,1,2}$ we performed a linear fit of the twelve parameters in (28) and (29) and looked for a minimum of the chi-square as a function of $\eta_{0,1,2}$. For the sea quark masses we imposed the relation $\chi_S = \sigma \chi_R$ and for the NLO-parameters the relations in (24) with the values of $\sigma_{1,2}$ given in Table 3. (The possible dependence of the NNLO-parameters $D$ and $Q$ on $\sigma$ has been neglected.) The minimum of the chi-square after the non-linear minimization is near

$$\eta_0 = 0.07, \qquad \eta_1 = 0.03, \qquad \eta_2 = 0.02. \tag{30}$$

The minimum as a function of $\eta_{0,1,2}$ is rather shallow but definitely within the bounds $0 \leq \eta_{0,1,2} \leq 0.10$. The minimization of the chi-square of the linear fit does not change

**Table 4.** Values of best fit parameters for the valence quark mass dependence. Quantities directly used in the fitting procedure are in bold face

| $\boldsymbol{\chi_R}$ | 33.5(2.4) | | |
|---|---|---|---|
| $\boldsymbol{\chi_R L_{R4W6}}$ | $5.24(38) \cdot 10^{-2}$ | $L_{R4W6}$ | $1.564(71) \cdot 10^{-3}$ |
| $\boldsymbol{\chi_R^2 Q_{nd}}$ | $6.5(1.8) \cdot 10^{-3}$ | $Q_{nd}$ | $5.80(79) \cdot 10^{-6}$ |
| $\boldsymbol{\chi_R L_{R5}}$ | $10.06(44) \cdot 10^{-2}$ | $L_{R5}$ | $3.00(19) \cdot 10^{-3}$ |
| $\boldsymbol{\chi_R^2 D_{fVV}}$ | $-9.3(1.7) \cdot 10^{-2}$ | $D_{fVV}$ | $-8.3(1.9) \cdot 10^{-5}$ |
| $\boldsymbol{\chi_R^2 Q_{fVV}}$ | $-2.80(19) \cdot 10^{-2}$ | $Q_{fVV}$ | $-2.50(50) \cdot 10^{-5}$ |
| $\boldsymbol{\chi_R^2 Q_{fVS}}$ | $-2.197(45) \cdot 10^{-2}$ | $Q_{fVS}$ | $-1.96(29) \cdot 10^{-5}$ |
| $\boldsymbol{\chi_R^2 Q_{fd}}$ | $-0.99(14) \cdot 10^{-2}$ | $Q_{fd}$ | $-0.89(45) \cdot 10^{-5}$ |
| $\boldsymbol{\chi_R L_{R85}}$ | $-2.10(12) \cdot 10^{-2}$ | $L_{R85}$ | $-6.25(52) \cdot 10^{-4}$ |
| $\boldsymbol{\chi_R^2 D_{nVV}}$ | $-1.67(20) \cdot 10^{-1}$ | $D_{nVV}$ | $-1.49(10) \cdot 10^{-4}$ |
| $\boldsymbol{\chi_R^2 Q_{nVV}}$ | $-8.44(67) \cdot 10^{-2}$ | $Q_{nVV}$ | $-7.53(48) \cdot 10^{-5}$ |
| $\boldsymbol{\chi_R^2 Q_{nVS}}$ | $-4.05(25) \cdot 10^{-2}$ | $Q_{nVS}$ | $-3.61(29) \cdot 10^{-5}$ |

the $\eta$ substantially: already the starting values are close to (30). This confirms the small value of $\eta_S$ found in our previous paper at $\beta = 4.68$ [9].

In contrast to the stable values of the $\eta$ there are large fluctuations in the basic parameter $\chi_R$: one can obtain values in the range $13 \leq \chi_R \leq 40$ depending on the set of functions fitted, on the fit interval etc. This is presumably the effect of our small number (only three) of sea quark masses. In order to obtain more stable results we fixed $\eta_{0,1,2}$ according to (30) and first determined in a linear fit the three parameters $\chi_R$, $\chi_R L_{R4W6}$ and $\chi_R^2 Q_{nd}$ from $RRn$. These parameters were then used as an input in the linear fit of the remaining nine parameters.

All 18 valence quark mass dependences considered can be reasonably well fitted. The best fit is shown by Figs. 1 and 2. The sum of the chi-squares of the linear fits is $\chi^2 \simeq 300$ for a number of degrees of freedom n.d.f. $= 18 \cdot 12 - 12 = 204$. Most of the chi-squares comes from the points with largest and smallest valence quark masses where there are obviously some systematic deviations, too. The parameters of best fit are given in Table 4. The values in the table show that there are some discrepancies in both relations in the last line of (17), but the deviations are not very large. The first and second relation give $-0.89(49) \cdot 10^{-5} \simeq 2.05(39) \cdot 10^{-5}$ and $0.52(9) \cdot 10^{-5} \simeq 0.92(8) \cdot 10^{-5}$, respectively.

The values of the NLO- and NNLO-parameters themselves are also shown in the right hand part of Table 4, with errors determined (as always) by the linearization method. With the help of the formulas in (5) and (6) one can also transfer these results to the corresponding $L$ and $W$ at some other renormalization scale different from $f_0\sqrt{\chi_R}$. Going to the conventional renormalization scale $\mu = 4\pi f_0$ and multiplying by an overall factor $128\pi^2$ one obtains the values of $\alpha_k$ and $\omega_k$ shown in Table 5.

Due to the unexpected smallness of the $\mathcal{O}(a)$ contributions it is interesting to try a linear fit of the valence quark mass dependences setting all $\mathcal{O}(a)$ terms to zero: $\eta_0 = \eta_1 = \eta_2 = 0$. This is a fit with eleven parameters because in the formulas $L_{S4W6}$ is always multiplied by $\eta_S$. The result is a reasonable fit but the chi-square is
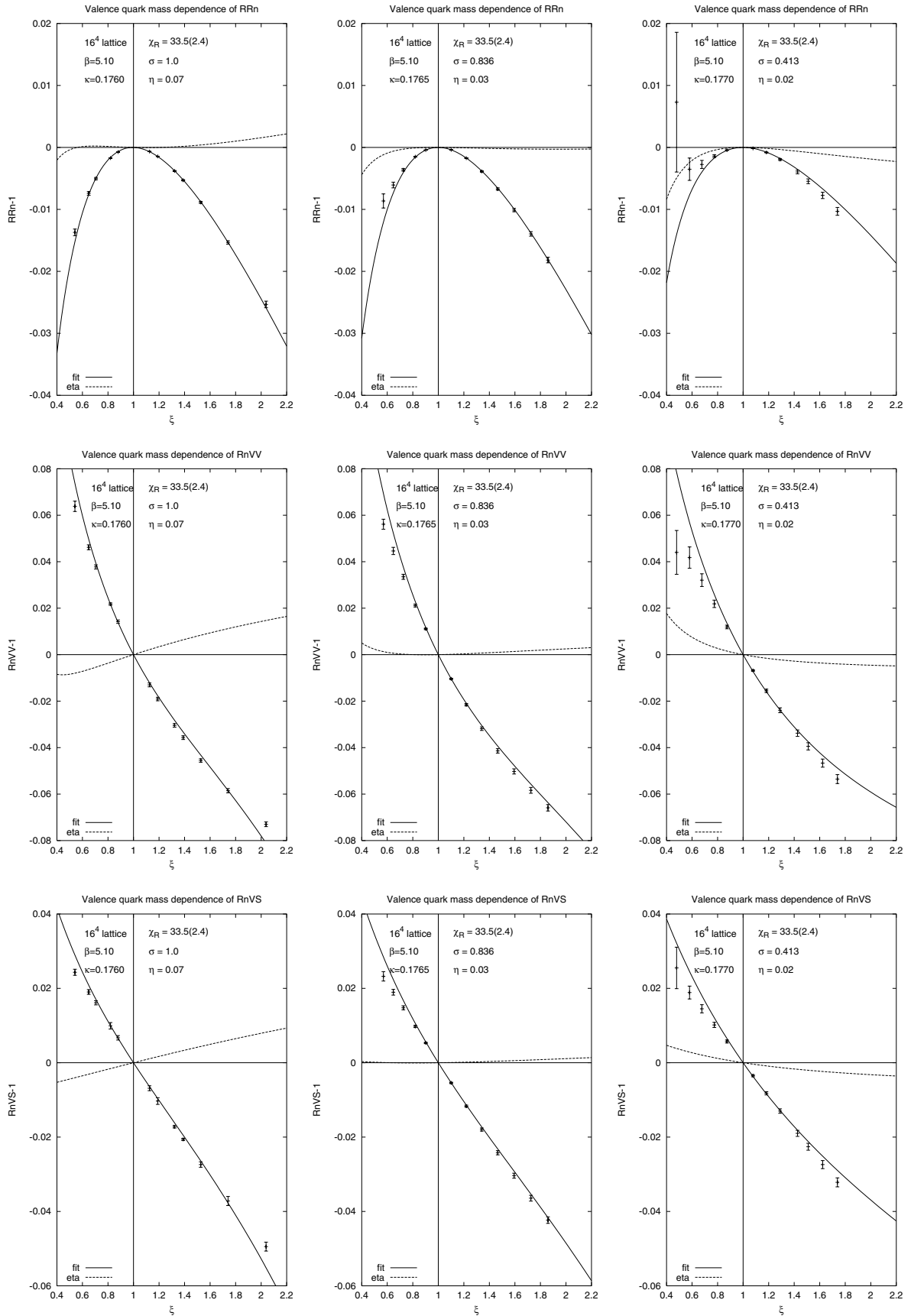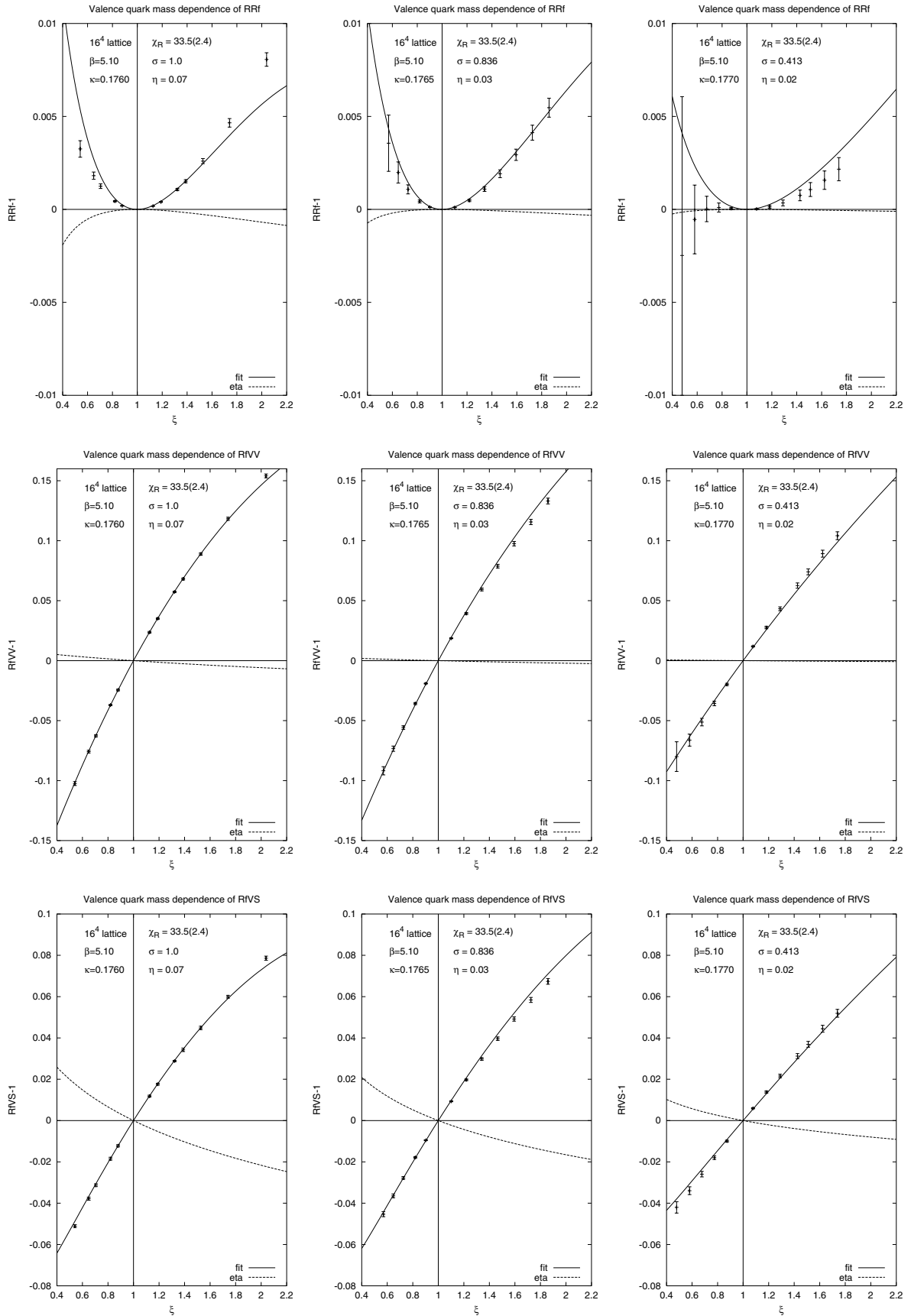
**Fig. 1.** $(RRn - 1)$, $(Rn_{VV} - 1)$ and $(Rn_{VS} - 1)$ for the three different sea quark mass values (full lines). Beside the fit the unphysical contribution (proportional to $\eta_S$) is separately shown (broken lines)

**Fig. 2.** $(RRf - 1)$, $(Rf_{VV} - 1)$ and $(Rf_{VS} - 1)$ for the three different sea quark mass values (full lines). Beside the fit the unphysical contribution (proportional to $\eta_S$) is separately shown (broken lines)

**Table 5.** Values of combinations of the $\alpha_k$ obtained from the best fit values in Table 4 and 6

| | | | | | |
|---|---|---|---|---|---|
| $\alpha_5$ | 2.24(20) | | | | |
| $\alpha_{85} \equiv (2\alpha_8 - \alpha_5)$ | 0.762(49) | | | $(\alpha_4 - \omega_6)$ | 2.36(9) |
| $\alpha_{45} \equiv (2\alpha_4 - \alpha_5)$ | 2.40(26) | $\Lambda_4/f_0$ | 22.9(1.5) | $\omega_{45}$ | $-1.7(1.8)$ |
| $\alpha_{6845} \equiv (4\alpha_6 + 2\alpha_8 - 2\alpha_4 - \alpha_5)$ | 0.658(86) | $\Lambda_3/f_0$ | 6.51(57) | $\omega_{6845}$ | $-5.43(60)$ |
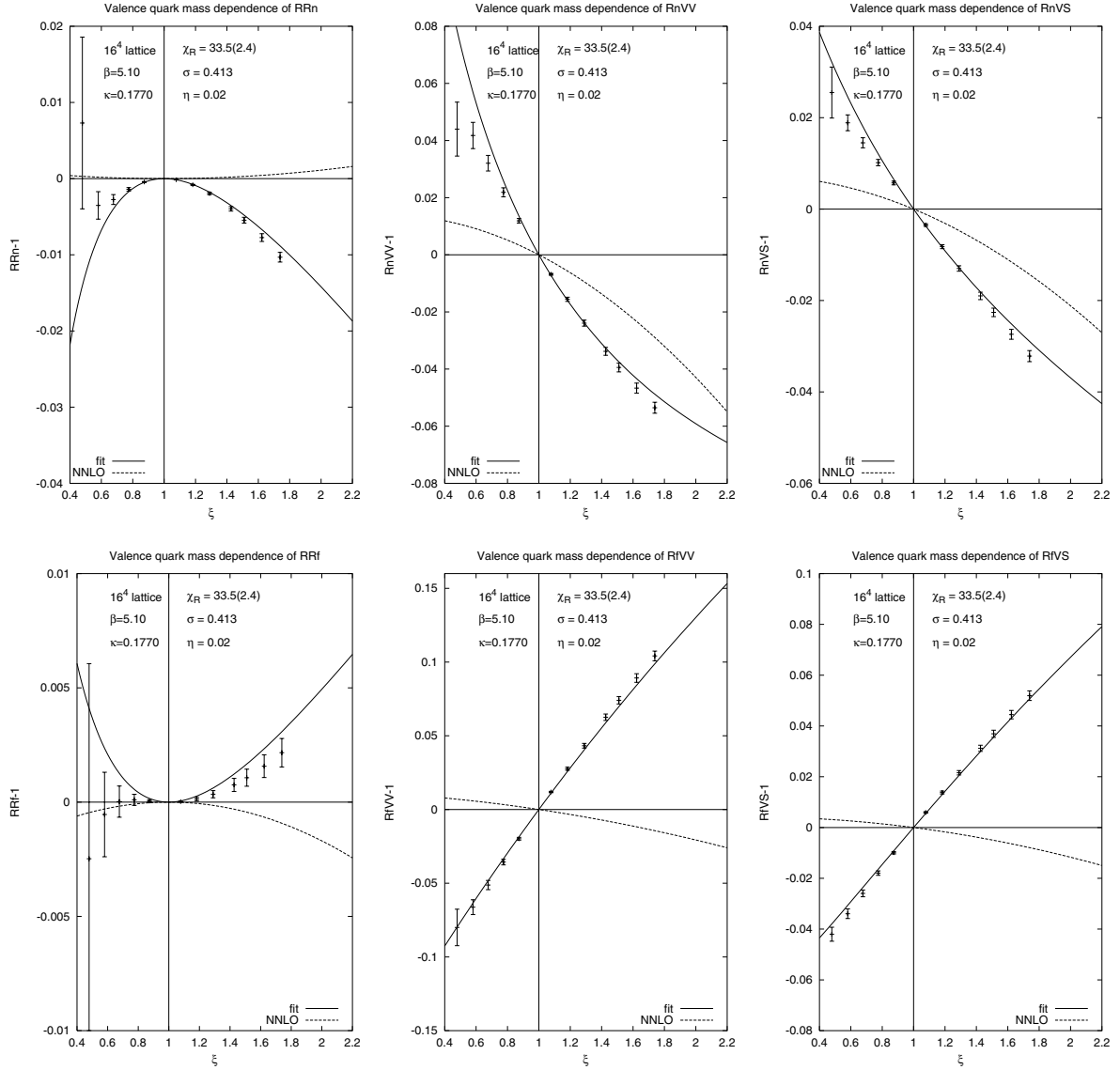


**Fig. 3.** NNLO tree-graph contribution at $\kappa_2 = 0.1770$ where the sea quark mass is given by $M_r \simeq 1$ (broken lines). The full lines represent the total fits shown also in Figs. 1 and 2 which are the sums of the continuum NLO, the $\mathcal{O}(a)$ and NNLO terms

by about 10% larger then in the case of $\eta_{0,1,2} \neq 0$. The best fit values of the main parameters are in this case $\chi_R = 36.1(1.0)$, $\alpha_5 = 2.08(14)$, $\alpha_{85} = 0.502(46)$.

The NNLO tree-graph contributions are rather important especially at $\kappa = 0.176$. From the point of view of the NLO formulas the situation becomes better at $\kappa = 0.177$ but NNLO is still not negligible there; see Fig. 3. (At $\kappa = 0.1765$ we have, of course, an intermediate situation

between $\kappa = 0.176$ and $\kappa = 0.177$.) In general, the NNLO contributions are more important in the ratios $R_{nVV}$ and $R_{nVS}$ than in $R_{fVV}$ and $R_{fVS}$. In fact, the ratios $R_{nVV}$ and $R_{nVS}$ at $\kappa = 0.176$ are dominated by NNLO. The relative importance of NNLO terms is stronger for $\xi > 1$ than for $\xi < 1$. In the double ratios $RRn$ and $RRf$ the NNLO terms are relatively unimportant.
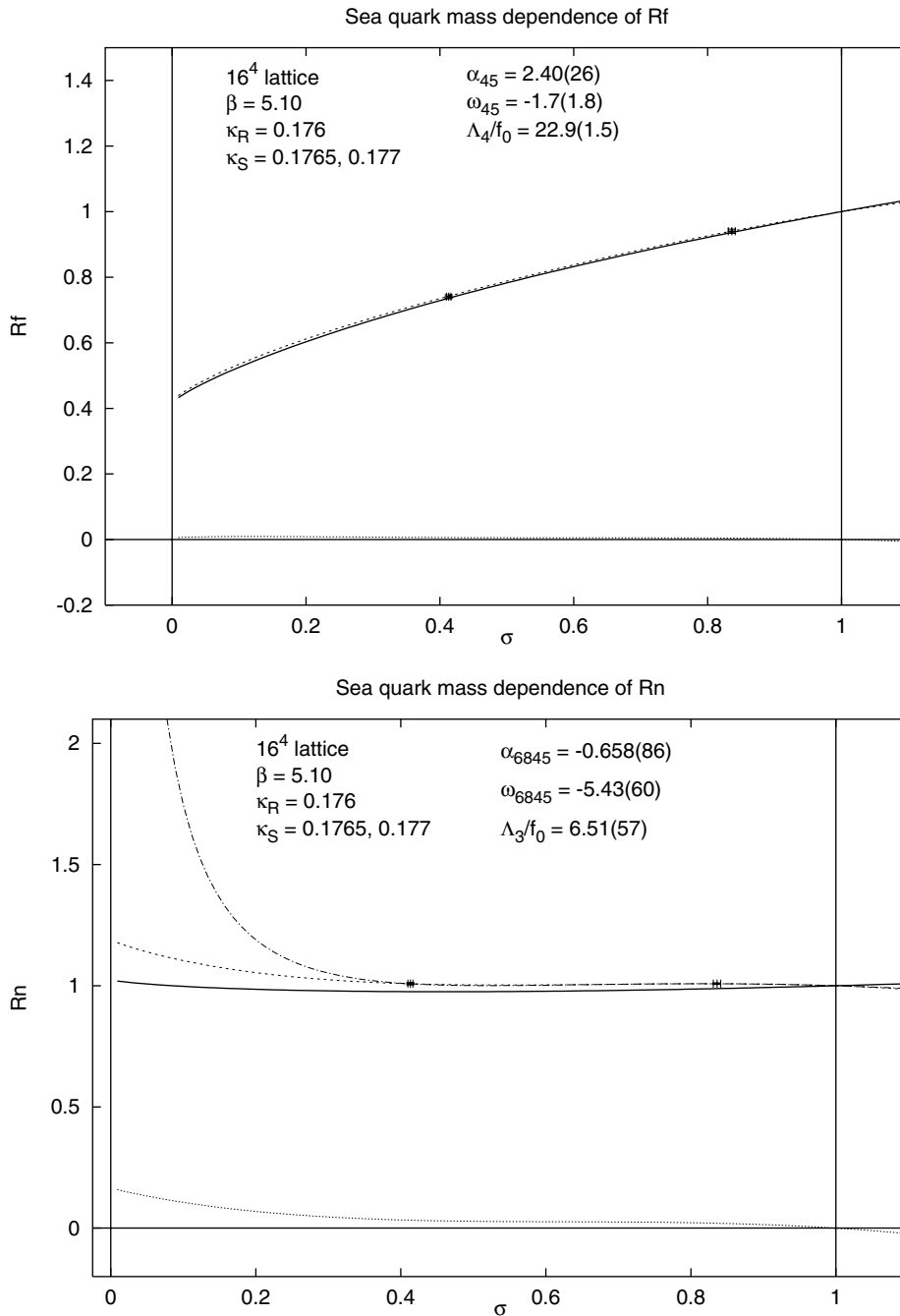
Sea quark mass dependence of Rf



Sea quark mass dependence of Rn



**Fig. 4.** $Rf_{\mathrm{SS}}$ and $Rn_{\mathrm{SS}}$. The full lines show the estimate of continuum contributions – without $\mathcal{O}(a)$ terms. The broken lines near zero show the unphysical contributions (proportional to $\eta_{\mathrm{S}}$). The other lines are different extrapolations of the measured values including $\mathcal{O}(a)$ terms (see text)

## 4.2 Sea quark mass dependence

The results from the fit of the valence quark mass dependence can also be used in the investigation of the sea quark mass dependence according to (22) and (23). In particular, the values (and errors) of $\chi_{\mathrm{R}}$ and $\eta_{0,1,2}$ are relevant there. Besides these values and the known ratios of the sea quark masses $\sigma_{1,2}$ (see Table 3) two extra parameter pairs appear, namely, for $N_{\mathrm{s}} = 2$,

$$L_{\mathrm{R45}} \equiv 2L_{\mathrm{R4}} + L_{\mathrm{R5}} , \quad W_{\mathrm{R45}} \equiv 2W_{\mathrm{R4}} + W_{\mathrm{R5}} \qquad (31)$$

in (22) and

$$L_{\mathrm{R6845}} \equiv 4L_{\mathrm{R6}} + 2L_{\mathrm{R8}} - 2L_{\mathrm{R4}} - L_{\mathrm{R5}} ,$$

$$W_{\mathrm{R6845}} \equiv 4W_{\mathrm{R6}} + 2W_{\mathrm{R8}} - 2W_{\mathrm{R4}} - W_{\mathrm{R5}} \qquad (32)$$

in (23).

Since we only have three sea quark mass values and therefore two independent values of $Rf_{\mathrm{SS}}$ and $Rn_{\mathrm{SS}}$ a "fit" actually means solving for the four unknowns. The results are collected in Table 6. The corresponding values of the

**Table 6.** Results for the parameters of the sea quark mass dependence. Quantities directly used in the fitting procedure are in bold face

| | | | |
|---|---|---|---|
| $\mathbf{L_{R45}}$ | $4.34(28) \cdot 10^{-3}$ | $Rf_{(\sigma=0)}$ | $0.415(19)$ |
| $\mathbf{W_{R45}}$ | $1.1(1.4) \cdot 10^{-3}$ | | |
| $\mathbf{L_{R6845}}$ | $-9.1(6.4) \cdot 10^{-5}$ | $Rn_{(\sigma=0)}$ | $1.025(17)$ |
| $\mathbf{W_{R6845}}$ | $-5.52(48) \cdot 10^{-3}$ | | |

$\alpha$ and $\omega$ are contained in Table 5. In this table also the values of the *universal low energy scales* $\Lambda_{3,4}$ are given. (For the definitions see [26, 27] or (10) in [9].) Once the parameters $L_{R45}$ and $L_{R6845}$ are known it is possible to extrapolate the continuum NLO curves (without the $\mathcal{O}(a)$ contributions) for $Rf_{SS}$ and $Rn_{SS}$ to zero sea quark mass; see Fig. 4. The values of these curves at $\sigma = 0$ are also given in Table 6.

The extrapolation of the full measured ratios, including $\mathcal{O}(a)$ contributions, requires an extrapolation of $\eta_S$ as a function of $\sigma$ which has, of course, a considerable uncertainty. The behavior of the extrapolated curve is especially sensitive to the assumed form of the $\eta_S$-extrapolation for $Rn_{SS}$ near zero. For instance, if the magnitude of the $\mathcal{O}(a)$ contribution given by $\rho_S = \eta_S \chi_S$ is finite at zero, which is reasonable to assume, then $Rn_{SS} = m_{SS}^2/(\sigma m_{RR}^2)$ has a $\sigma^{-1}$ singularity near zero. This is a manifestation of the fact that different definitions of the "critical line" in the $(\beta, \kappa)$-plane, for instance by $m_\pi^2 = 0$ or $m_q^{PCAC} = 0$, in general differ by lattice artifacts (in our case by $\mathcal{O}(a)$). If, however, $\eta_S = \rho_S/\chi_S$ would have a finite value at $\sigma = 0$ then there would be no such singularity. The two extrapolations shown in the lower part of Fig. 4 are examples of these two cases.

Concerning the results on the parameters obtained from the sea quark mass dependence (Table 6 and the second half of Table 5) one has to remark that the assumption of a quark mass independent lattice spacing $a$ has an important effect on them. Assuming a quark mass independent Sommer scale parameter $r_0$ would change these results substantially. (There would be small changes in the first half of Table 5 due to the somewhat different values of the quark mass ratios $\sigma_{1,2}$, too.) For instance, the values of $\Lambda_4/f_0$ and $\Lambda_3/f_0$ would come out to be 16.1(1.1) and 30.4(2.9), respectively, instead of the values given in the tables. As it has been discussed above, the choice of a quark mass independent renormalization scheme requires a quark mass independent lattice spacing and is not consistent with a quark mass independent $r_0$ [25,28]. Nevertheless, it is plausible that in the continuum limit and in the limit of very small sea quark masses $r_0/a$ becomes independent from the sea quark mass and the differences between the values for constant $r_0$ and $a$ disappear.

# 5 Summary and discussion

The results obtained in this paper for the Gasser–Leutwyler constants (see Tables 4, 5 and 6) can only be taken as estimates of the values in continuum. In order to deduce continuum values with controlled error estimates the left out lattice artifacts have to be removed by performing simulations at increasing $\beta$ values and extrapolating the results to $a = 0$. Reasonable next steps would be to tune the lattice spacing to $a \simeq 0.13$ fm on $24^3 \cdot 48$ and $a \simeq 0.10$ fm on $32^3 \cdot 64$ lattices. This would require with the TSMB algorithm by a factor of about 10 and 100 more computer time, respectively. Our calculations near $a \simeq 0.20$ fm should be improved by going from $16^4$ to $16^3 \cdot 32$ lattices in order to improve the extraction of the physical quantities of interest. The number of sea quark masses considered should be increased to 5–6 towards smaller values. This will decrease the overall statistical errors considerably. We hope to reach sea quark masses about $m_{sea} \simeq \frac{1}{6} m_s$ on $16^3 \cdot 32$ lattices in the near future.

General conclusions of the present work are the following.
(1) Compensating $\mathcal{O}(a)$ effects in the pseudo-Goldstone boson sector by introducing $\mathcal{O}(a)$ terms in the PQCh-Lagrangian itself is a viable alternative to the $\mathcal{O}(a)$-improvement of the lattice action. An extension to also treat $\mathcal{O}(a^2)$ effects in the PQCh-Lagrangian is possible [20, 21] and has been partially taken into account also in the present paper.
(2) The observed $\mathcal{O}(a)$ contributions in the pseudo-Goldstone boson sector are surprisingly small. The ratios of the $\mathcal{O}(a)$-parameters in the NLO PQCh-Lagrangian to the quark masses $\eta_S \equiv \rho_S/\chi_S$ are in our present range of quark masses ($\frac{1}{3} m_s \leq m_{sea} \leq \frac{2}{3} m_s$) at the few percent level.
(3) Taking ratios of pion mass squares and pion decay constants at fixed gauge coupling and varying quark masses has the advantage that the $Z$-factors of multiplicative renormalization as well as all sorts of quark mass independent corrections cancel.
(4) NNLO contributions in PQChPT are in our present sea quark mass range rather important. In fact, they are more important than the $\mathcal{O}(a)$ lattice artifacts. This introduces new parameters in the multi-parameter fits which makes the fitting procedure more difficult. The situation will be better at smaller sea quark masses where the importance of NNLO terms diminishes.

The present results strengthen the observation already made in our previous paper [9] that the expected behavior dictated by PQChPT sets in rather early – at relatively large lattice spacings – once the quark masses are small enough. Our present cut-off $a^{-1} \simeq 1$ GeV is already a "high energy scale" from the point of view of the pion dynamics. As a consequence, it seems to us that the numerical study of the pseudo-Goldstone boson sector of QCD is perhaps the easiest field for obtaining new quantitative results about hadron physics by lattice simulations.

We thank Steve Sharpe for correspondence on the structure of the NNLO terms in the PQChPT formulas and Marteen Golterman and Oliver Bär for helpful discussions. We thankfully acknowledge the contributions of Claus Gebert in the early stages of this work.

## References

1. S. Weinberg, Phys. Rev. **166**, 1568 (1968)
2. J. Gasser, H. Leutwyler, Annals Phys. **158**, 142 (1984)
3. ALPHA Collaboration, J. Heitger et al., Nucl. Phys. B **588**, 377 (2000), hep-lat/0006026
4. UKQCD Collaboration, A.C. Irving et al., Phys. Lett. B **518**, 243 (2001), hep-lat/0107023
5. G.T. Fleming, D.R. Nelson, G.W. Kilcup, Nucl. Phys. Proc. Suppl. **106**, 221 (2002), hep-lat/0110112
6. G.T. Fleming, D.R. Nelson, G.W. Kilcup, hep-lat/0209141
7. qq+q Collaboration, F. Farchioni, C. Gebert, I. Montvay, L. Scorzato, Eur. Phys. J. C **26**, 237 (2002), hep-lat/0206008
8. qq+q Collaboration, F. Farchioni, C. Gebert, I. Montvay, L. Scorzato, hep-lat/0209142
9. qq+q Collaboration, F. Farchioni, C. Gebert, I. Montvay, E. Scholz, L. Scorzato, Phys. Lett. B **561**, 102 (2003), hep-lat/0302011
10. I. Montvay, Nucl. Phys. B **466**, 259 (1996), hep-lat/9510042
11. C.W. Bernard, M.F.L. Golterman, Phys. Rev. D **49**, 486 (1994), hep-lat/9306005
12. S.R. Sharpe, Phys. Rev. D **56**, 7052 (1997), hep-lat/9707018, Erratum D **62**, 099901 (2000)
13. M.F.L. Golterman, K.-Ch. Leung, Phys. Rev. D **57**, 5703 (1998), hep-lat/9711033
14. S.R. Sharpe, N. Shoresh, Phys. Rev. D **62**, 094503 (2000), hep-lat/0006017
15. B. Sheikholeslami, R. Wohlert, Nucl. Phys. B **259**, 572 (1985)
16. G. Rupak, N. Shoresh, Phys. Rev. D **66**, 054503 (2002), hep-lat/0201019
17. JLQCD Collaboration, S. Hashimoto et al., hep-lat/0209091
18. JLQCD Collaboration, S. Aoki et al., Nucl. Phys. Proc. Suppl. **106**, 224 (2002), hep-lat/0110179
19. S.R. Sharpe, R. Van de Water, poster presented at the Tsukuba Lattice Conference 2003, to be published in the Proceedings, hep-lat/030810
20. O. Baer, G. Rupak, N. Shoresh, hep-lat/0306021
21. S. Aoki, hep-lat/0306027
22. C. Gebert, Ph.D. Thesis, Hamburg University, 2002
23. ALPHA Collaboration, R. Frezzotti, M. Hasenbusch, U. Wolff, J. Heitger, K. Jansen, Comput. Phys. Commun. **136**, 1 (2001), hep-lat/0009027
24. U. Wolff, hep-lat/0306017
25. S. Aoki, Nucl. Phys. Proc. Suppl. **94**, 3 (2001), hep-lat/0011074
26. S. Dürr, hep-lat/0208051
27. H. Leutwyler, Nucl. Phys. Proc. Suppl. **94**, 108 (2001), hep-ph/0011049
28. R. Sommer, talk presented at the Tsukuba Lattice Conference 2003, to be published in the Proceedings